On the structural behaviour of existing RC bridges subjected to corrosion effects: numerical insight

Marco ZUCCA[(1)*], Emanuele RECCIA[(1)], Nicolo LONGARINI[(2)], Victor EREMEYEV[(1)], Pietro CRESPI[(2)]

(1) Department of Civil, Environmental Engineering and Architecture
University of Cagliari, Italy
(2) Department of Architecture, Built Environment and Construction Engineering
Politecnico di Milano, Milano, Italy
** Corresponding author. E-mail: marco.zucca2@unica.it*

Abstract

The evaluation of the structural behaviour of existing reinforced concrete (RC) bridges represents one of the most current structural engineering research topics due to their strategic importance, especially if they are subjected to corrosion effects which can lead to a significant reduction of load-bearing capacity of the main structural elements (e.g., the piers). In the last decades, different types of numerical approaches have been proposed for the evaluation of the structural behaviour of these strategic infrastructures, especially after the recent collapses that have affected this type of structures during last years. In this paper, the structural behaviour of an existing RC bridge subjected to corrosion effects due to carbonation is analysed by means of an efficient procedure based on the implementation of a Finite Element Model (FEM) where the main structural elements are implemented using only Timoshenko beam elements. The safety level of the bridge has been evaluated considering different load conditions (e.g. traffic load, seismic action, etc.) calculated according to the Italian Design Code (NTC2018). Finally, a retrofitting intervention is proposed in order to guarantee and adequate safety level of the bridge under the considered different load combinations.

Keywords*: existing RC bridge; corrosion effects; carbonation phenomenon; non-linear analyses.*

1. Introduction

During last decades, the evaluation of the structural behaviour of existing reinforced concrete (RC) bridges has attracted increasing attention in the scientific community and in the designers also considering several collapses that have occurred due to incorrect scheduling of the maintenance interventions [1-4]. One of the most important aspects which influence the load-bearing capacity of existing RC bridges is the presence of the corrosion effects that affect the main structural elements [5-9]. For this reason, several researchers have been proposed different approaches to evaluate the influence of the corrosion effects on the load-bearing capacity of existing RC bridges both under vertical and horizontal loads [10-13]. In [14] an efficient procedure for the evaluation of the structural behaviour of existing RC bridges subjected to corrosion effects due to carbonation under horizontal loads has been presented. The obtained results showed that the decrease of the load-bearing capacity is strictly related to the considered corrosion scenario as a function of the age of the bridge. Gardoni et al. [15] have developed a Bayesian approach useful to obtain the seismic fragility curves of the bridge components subjected to corrosion effects. In particular, the approach has been applied to two existing RC bridges to evaluate their sensitivity to corrosion effects. In [16] a simplified approach useful to obtain the maintenance interventions period of existing motorway RC viaducts considering the age of the structure has been proposed taking into account three different corrosion scenarios (slight, moderate and high). In this research work, corrosion effects have been modelled considering a uniform corrosion distribution along the piers with a consequent reduction of steel reinforcements area. In Pelle et al. [17] the corrosion effects induced by the chlorides acting on the RC bridge piers have been analysed considering the possible achievement of buckling phenomena of the longitudinal steel reinforcements. Kumar et al. [18] investigated the effect of cumulative seismic damage and corrosion on the life cycle cost of existing RC bridges highlighting that both phenomena significantly influence the collapse mechanisms to which an existing RC bridge may be subjected. Ou et al. [19] have been evaluated the long-term seismic performance of existing RC bridges subject to corrosion phenomena due to the presence of chloride. A sensible reduction of the PGA value which leads to the collapse of the first structural element has been observed especially for bridges adjacent to a coastline. In Fan et al. [20] the structural performance of RC bridges under multi-hazard effect of vessel impact and corrosion has been studied, determining that corrosion deterioration has a significant influence on the vessel-impact performance of bridge structures. Yuan et al [21] have analysed the different collapse mechanisms of RC concrete costal bridge piers considering the effects of corrosion-induced damage. Moreover, in Yuan et al [22] a series of shaking table tests have been performed to evaluate the structural performance of coastal bridge piers with different levels of corrosion damage caused by chloride penetration. Ma et al [23] analysed the seismic behaviour of thirteen corroded circular piers through cyclic loading tests. The results showed that a higher corrosion level could cause a more obvious deterioration of the structural strength, stiffness, ductility, and energy dissipation capacity. A brittle failure has been obtained for several specimens, owing to the severe damage of stirrups and a high axial load. In Lin et al [24] the dynamic behaviour of RC frames subject to corrosion effect has been studied via the shaking table test. The results obtained have shown the important effects of steel reinforcement corrosion on the response of the displacement, acceleration, and spectral curve of the structures.

Focusing attention on the current literature, other several researchers have been evaluated the correlation between the corrosion effects of the main structural elements of the bridges and their structural performance [25-34].

In this paper the evaluation of the structural behaviour of an existing RC bridge built in 1973 and located in Northern Italy is discussed. In particular, the bridge analysed is characterized by one carriageway composed by 24 simply supported 36.61 m spans and 23 piers where three of these are subjected to significant corrosion effects due to carbonation which interested the longitudinal steel reinforcements and the stirrups. Several scenarios which involve different load cases, defined according to [35], are presented in order to define the correct maintenance interventions useful to

guarantee an adequate safety level of the bridge under vertical and horizontal loads. In particular, the manuscript is organized as follows: after a brief introduction (Section 1), the structural modelling technique used in this research work is described in detail in Section 2. Section 3 reports the description of the case study and the discussion of the results obtained from the execution of the linear and non-linear numerical analyses. Finally, in Section 4 the main conclusions, based on the results obtained and described in previous Section 3, have been summarized.

2. Structural modelling

To evaluate the structural behaviour of existing RC bridges, an efficient procedure based on the implementation of simplified Finite Element Models (FEMs) through MIDAS Civil [36] software has been used where the main structural elements of the bridges (piers, pier caps and deck) have been modelled only with Timoshenko beam elements in order to reduce the computational effort [14]. Furthermore, the elastomeric bearings have been introduced in the FEM using general elastic links connected to the pier cap and the deck with a system of rigid links. The translational and rotational stiffnesses of the elastic links representing the elastomeric bearings have been calculated considering as reported in [37]. The abutments are considered as perfect restraints applied at the base node of the elastic links representing the elastomeric bearings located at the deck-abutment interface. Also, the foundation of the piers has been implemented as perfect restraints applied at the node in correspondence to the base of each pier.
To evaluate the correct dynamic behaviour of the existing RC bridges, the reduction of the gross-section bending stiffness of the piers due to concrete cracking is introduced considering appropriate scale factors calculated according to [38], evaluated starting from the related moment-curvature (M-χ) diagram. On the contrary, the stiffness of the deck is not reduced considering that during a seismic event remain within the elastic range [6,39]. During the evaluation of the dynamic behaviour of the bridges, the influence of structural and non-structural masses has been considered while the traffic load has been neglected according to as reported in [35].
Two collapse mechanisms of the piers have been monitored: (i) the ductile failure mechanism which is related to the gross-section moment-curvature diagram and characterized by an initial elastic phase followed by a large strain hardening plastic behaviour and (ii) the brittle failure mechanism that is regulated by the shear strength of the considered structural element. The ductile failure mechanism is based on the rotational capacity of the plastic hinge while the brittle mechanism is governed by the shear strength of the pier (V_R) calculated considering the formulation proposed by [40] for the cyclic shear resistance. The materials non-linear behaviour is modelled taking into account the Kent and Park model (Fig. 1a) [41] for the concrete and the Park Strain Hardening constitutive law (Fig. 1b) [42] for the steel reinforcements.

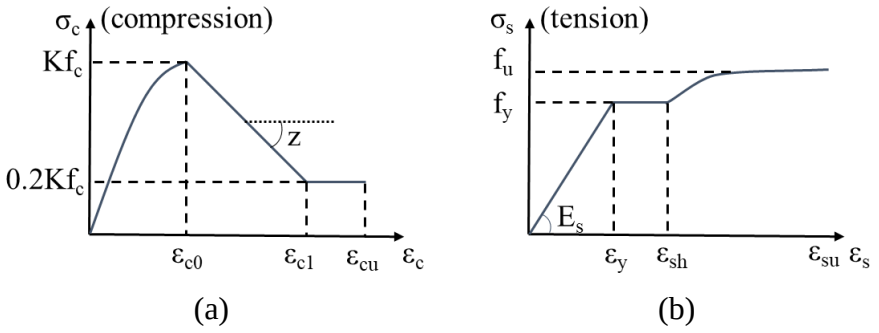

Figure 1. (a) Kent and Park and (b) Park Strain Hardening model.

The non-linear behaviour of the structure is introduced in the FEM through the application of appropriate plastic hinges located in correspondence to the element at the base of each pier where the activation of the ductile collapse mechanism is hypothesized. The properties of the plastic hinges have been obtained considering as reported in [43,44] both for ductile and brittle collapse mechanism (Fig. 2).

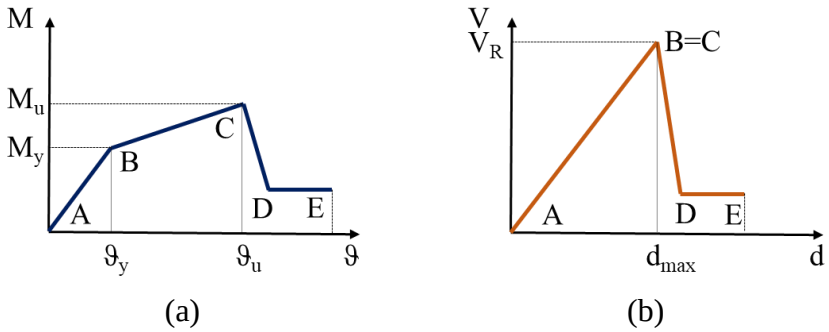

Figure 2. Definition of (a) ductile and (b) brittle failure mechanism.

The verification criteria adopted in this work are the following: for the ductile collapse mechanism, the achievement of the ¾ of the ultimate rotation ϑ_u (C point in Fig. 2a) while for the brittle failure mechanism, the overcome of the above-mentioned shear resistance V_R (B=C point in Fig. 2b).
As mentioned in previous Section 1, the bridge analysed was built in 1973 and 3 of the 24 piers showed the presence of significant corrosion effects due to carbonation which involves both longitudinal and transverse steel reinforcements. In particular, carbonation happens when the carbon dioxide in air penetrates into the concrete volume and reacting with hydroxides, generating carbonates. This phenomenon led to a pore solution pH reduction below the value of 8.5 resulting in an unstable passive film protecting the surface of steel rebars. It possible to define two main phases of the corrosion process development: initiation and propagation.
Eq. 1 shows the penetration law in a generic concrete volume (which defines the first phase) regulated by a parabolic trend [45-47]:

$$s = k \cdot t^{1/n} \tag{1}$$

where s represents the thickness of the carbonated concrete layer that depends on the penetration rate coefficient k and the time t. As mentioned before, the structure was built around the 1970's and consequently the parameter n, which depends on the concrete characteristics, is taken equal to 2 for normal compacted concrete. To introduce the corrosion effects due to carbonation in the structural modelling, a simplified analytical model which define the reduction of the longitudinal and transverse steel reinforcements area has been adopted. The reduction of steel reinforcements diameter and area is calculated following Eq. 2 and 3, respectively.

$$d(t) = d_0 - 2P(t) = d_0 - 2i_{corr}k(t - t_i), \tag{2}$$

$$A_s(t) = \pi[d_0 - 2i_{corr}k(t - t_i)]^2/4, \tag{3}$$

where t indicates the bridge age, k the penetration rate coefficient in mm/year$^{0.5}$ and i_{corr} the mean corrosion current density expressed in μA/cm^2. It is possible to notice that the variation of the steel reinforcements diameter d and area A_s depends on the corroded thickness P(t). Table 1 summarizes

the parameters used for the execution of the numerical analyses, where f_{ck} is the characteristic cylinder concrete compressive strength, i_{corr} is the value of the corrosion current density taking into consideration a high corrosion scenario defined according to [48], t_i is the initiation time taken equal to 13.5 years [49], k is the penetration rate coefficient and $\varepsilon_{u,0}$ is the ultimate tensile strain of the steel reinforcements.

Table 1. Corrosion parameters.

f_{ck} [MPa]	i_{corr} [μA/cm^2]	t_i [year]	k [-]	$\varepsilon_{u,0}$ [%]
28	5	13.5	0.0116	2

Other several models are proposed in literature to evaluate the corrosion effects due to carbonation on the load-bearing capacity of R.C. structures [50,51], but appear more complex to use during design phase.

3. Case study

The structural behaviour of an existing RC bridge located in Northern Italy and built in 1973 has been analysed. In particular, the bridge is characterized by one carriageway composed by 24 simply supported spans which create a linear altimetric layout with a curved planimetric trend. The overall width of the of the roadway is about 10.47 m and each span consist of a precast concrete slab of four prestressed I girders (Fig. 3). The deck is made by a concrete slab 20 cm thick. Each span is supported by 4 x 2 elastomeric bearings located in correspondence to the hammer cap.

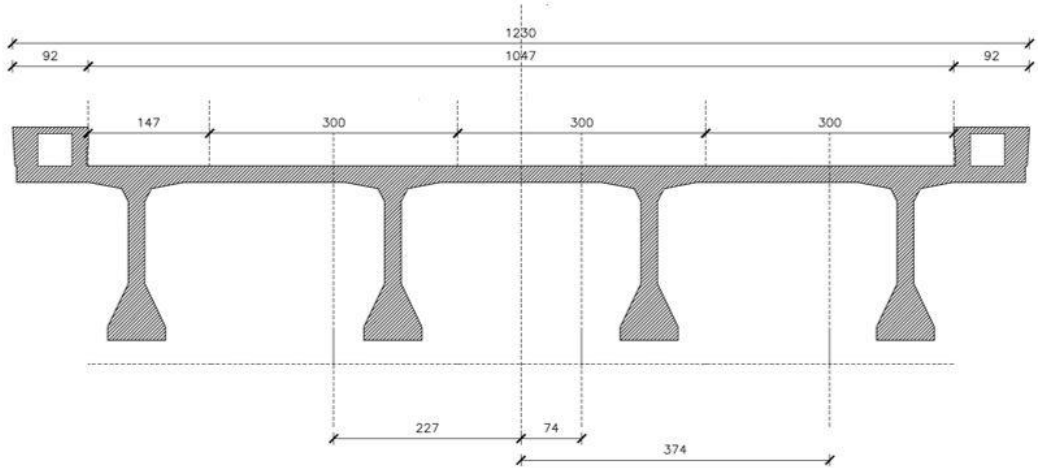

Figure 3. Deck cross-section (measures in cm).

The first twenty piers are characterized by a hollow octagonal cross-section with a height ranging between 9.12 m and 67.63 m while the other three piers are characterized by a rectangular section and by a height ranging between 2.61 m and 4.73 m. The bridge is made with f_{ck} = 28 MPa concrete and f_{yk} = 440 MPa steel.
Fig. 4 shows the FEM of the bridge while Tables 2 and Fig. 5 report, respectively, the main structural properties of the RC piers and the related cross-section.

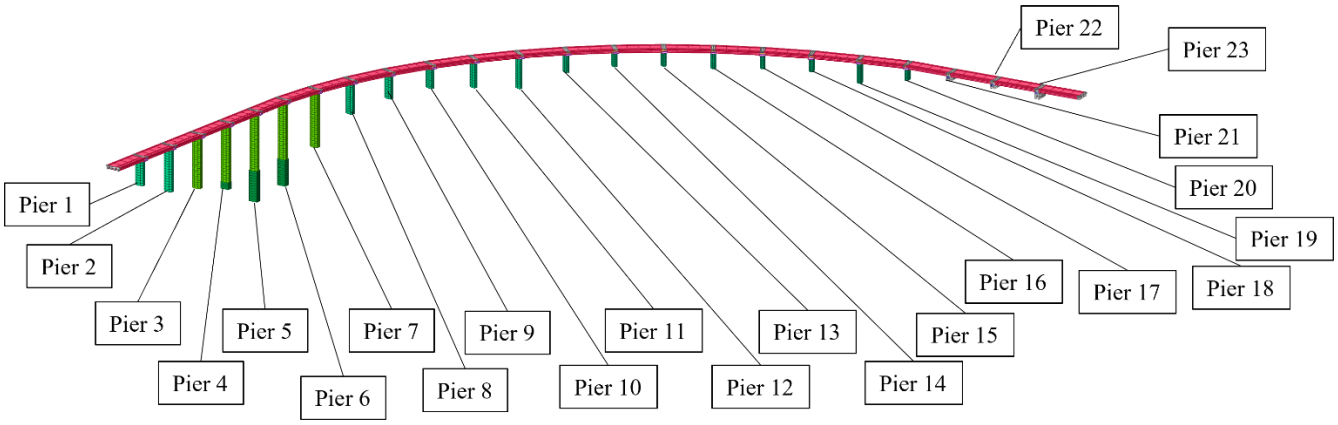

Figure 4. FEM of the bridge.

Table 2. Main structural characteristics of the piers.

Pier [n°]	Pier shape [-]	Height [m]	Cross-section dimensions [m]	Pier thickness [m]	Longitudinal steel reinforcement [-]	Stirrups [-]
1	Octagonal hollow	19.48	6.8 x 3.6	0.25	116Ø20	Ø8/20
2	Octagonal hollow	33.28	6.8 x 3.6	0.25	116Ø20	Ø8/20
3	Octagonal hollow	39.58	6.8 x 3.6	0.25	116Ø20	Ø8/20
4	Octagonal hollow	48.97	6.8 x 3.6	0.25	116Ø20	Ø8/20
5	Octagonal hollow	67.63	6.8 x 3.6	0.25	116Ø20	Ø8/20
6	Octagonal hollow	64.11	6.8 x 3.6	0.25	116Ø20	Ø8/20
7	Octagonal hollow	42.35	6.8 x 3.6	0.25	116Ø20	Ø8/20
8	Octagonal hollow	23.78	6.8 x 3.6	0.25	116Ø20	Ø8/20
9	Octagonal hollow	18.19	6.8 x 3.6	0.25	116Ø20	Ø8/20
10	Octagonal hollow	15.64	6.8 x 3.6	0.25	116Ø20	Ø8/20
11	Octagonal hollow	19.71	6.8 x 3.6	0.25	116Ø20	Ø8/20
12	Octagonal hollow	23.96	6.8 x 3.6	0.25	116Ø20	Ø8/20
13	Octagonal hollow	15.20	6.8 x 3.6	0.25	116Ø20	Ø8/20
14	Octagonal hollow	10.95	6.8 x 3.6	0.25	116Ø20	Ø8/20
15	Octagonal hollow	11.00	6.8 x 3.6	0.25	116Ø20	Ø8/20
16	Octagonal hollow	12.31	6.8 x 3.6	0.25	116Ø20	Ø8/20
17	Octagonal hollow	10.61	6.8 x 3.6	0.25	116Ø20	Ø8/20
18	Octagonal hollow	10.40	6.8 x 3.6	0.25	116Ø20	Ø8/20
19	Octagonal hollow	15.80	6.8 x 3.6	0.25	116Ø20	Ø8/20
20	Octagonal hollow	9.12	6.8 x 3.6	0.25	116Ø20	Ø8/20
21	Rectangular	2.94	10.7x1.0	-	166Ø16	Ø8/20
22	Rectangular	2.61	10.7x1.0	-	166Ø16	Ø8/20
23	Rectangular	4.73	10.7x1.0	-	166Ø16	Ø8/20

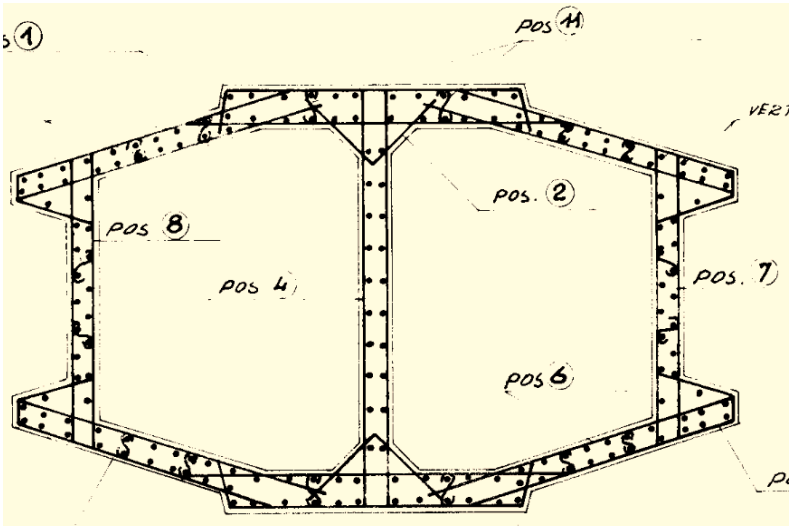

Figure 5. Cross-section of the bridge piers.

Considering as reported in Table 2, it is possible to notice that the bridge is characterized by poor construction details typical of the RC bridges built in Italy around the 1970's, especially regarding the stirrups because they are designed to resist to low value of horizontal action.
As mentioned before, the piers 4, 5 and 6, located near a valley, are subjected to significant corrosion effects due to carbonation (Fig. 6) and for this reason four different scenarios have been analyzed to evaluate the structural behavior of the bridge:

- scenario 0, where the structural analyses has been carried out without taking into account the corrosion effects;
- scenario 1, where the corrosion effects have been applied to all the steel reinforcements of the piers 4, 5 and 6;
- scenario 2, where the corrosion effects have been considered acting only in the steel reinforcements positioned in the inner perimeter of the hollow octagonal cross-section of the piers 4, 5 and 6 while the steel reinforcements of the outer perimeter are not considered in the structural verifications;
- scenario 3, where the steel reinforcements of the inner perimeter of the hollow octagonal cross-section of the piers 4, 5 and 6 are not considered affected by corrosion effects and those of the outer perimeter are not taken into account during the execution of the structural verifications.

The structural behavior of the bridge has been evaluated considering two different configurations: (i) current configuration and (ii) transient design situation (Fig. 7). These two configurations differ in the application of traffic loads which in current configurations are considered acting in all the three lanes while in transient configuration the application of the traffic loads is limited to two lanes. In particular, for the current configuration scenarios 0, 1 and 2 have been considered while for the transient configuration the analyses have been carried out taking into account scenarios 2 and 3.
Table 3 summarizes the steel reinforcements diameter reduction, calculated through previous Eq. 2 where t is fixed equal to 50 years and i_{corr} is taken equal to 5 $\mu A/cm^2$ as indicated for high corrosion level in [48].

Figure 6. Piers 5 and 6.

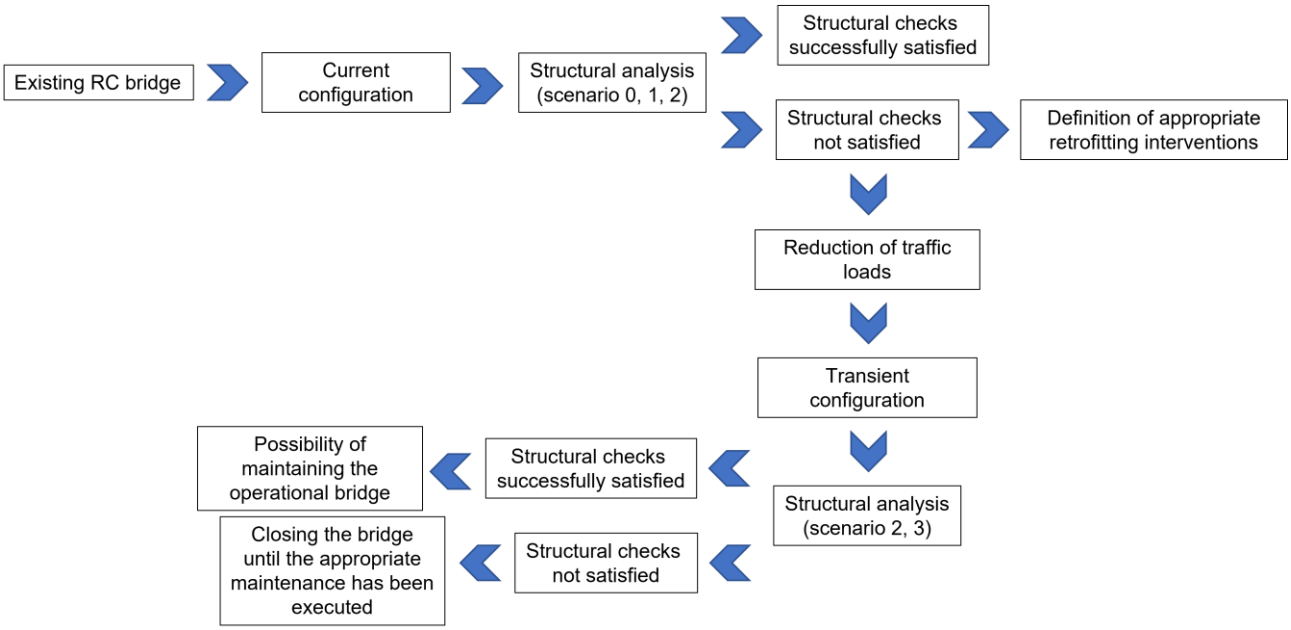

Figure 7. Flow chart of the present work.

Table 3. Steel reinforcements diameter reduction.

d_0 [mm]	d [mm]	Δd [%]
8	4.5	44.2
16	12.5	22.1
20	16.5	17.7

3.1 Current configuration

The structural analyses of the bridge considering the current configuration have been performed starting from the implementation of a simplified FEM (composed by 801 Timoshenko beam elements) as described in previous Section 2 and considering the presence of traffic loads calculated as reported in [35]. Furthermore, the seismic action has been calculated based on the seismic parameters of the site where the bridge was built and reported in Table 4 where V_N is the life of the structure, U_C is the use category, C_u is the coefficient for use category, V_R is the reference life, P_{VR} is the probability of exceedance (related to the considered limit state), S_T is the topographic coefficient, S_C is the soil category and PGA indicates the value of the design peak ground acceleration.

Table 4. Main seismic parameters of the site.

V_N [year]	U_c [-]	C_u [-]	V_R [year]	P_{VR} [%]	S_T [-]	Sc [-]	PGA [g]
50	IV	2	100	10	1	C	0.068

In first approach, linear dynamic analysis has been carried out considering a behaviour factor equal to q = 1.5. As mentioned before, the load combinations have been defined according to as reported in [35].
Table 5 summarizes the range of the safety indices obtained for piers 4, 5, and 6 calculated considering the different load combinations and where S_{c0}, S_{c1} and S_{c2} indicate scenario 0, 1 and 2, respectively. Values of safety index close or greater than one characterizes cases where the security level is not adequate.

Table 5. Range of the safety indices obtained for the current configuration considering the load combinations defined according to [35].

Pier 4			Pier 5			Pier 6		
Sc0	Sc1	Sc2	Sc0	Sc1	Sc2	Sc0	Sc1	Sc2
[-]	[-]	[-]	[-]	[-]	[-]	[-]	[-]	[-]
0.11-0.68	0.12-0.76	0.18-0.88	0.11-0.70	0.12-0.80	0.17-1.08	0.09-0.85	0.09-1.03	0.14-1.50

The results show that the safety indices obtained for the pier 4 are characterized by values less than one, but still close to one considering the scenario 2. Pier 5 is characterized by maximum value of safety indices greater than one in the case of scenario 2 and equal to 0.8 for the scenario 1. The higher values of safety indices are obtained for the piers 6 where reach 0.85, 1.03 and 1.5 for the scenario 0, 1 and 2, respectively, considering the ductile collapse mechanism. Instead, it is important to highlight that the lower values of the safety indices obtained are related to the serviceability limit state.
Based on the values of safety indices above illustrated, a reduction of the traffic load has been hypothesized (transient configuration) to understand if in this configuration the temporary operation of the bridge can be guaranteed.

3.2 Transient configuration

As mentioned in previous Section 2, the transient configuration differs from the current one, described in Section 3.1, for the traffic loads considered applied at two of the three lanes. In this case, for the execution of the structural analyses, scenarios 2 and 3 have been taken into account. The applied loads and their combinations are the same considered for the current configuration. Table 6 reports the range of the safety indices calculated for the two analysed scenarios.

Table 6. Range of the safety indices obtained for the transient configuration considering the load combinations defined according to [35].

Pier 4		Pier 5		Pier 6	
Sc2	Sc3	Sc2	Sc3	Sc2	Sc3
[-]	[-]	[-]	[-]	[-]	[-]
0.15-0.74	0.14-0.69	0.14-1.00	0.13-0.93	0.11-1.00	0.10-0.94

It is possible to notice that, also in this case, the lower values of safety indices calculated are related to the serviceability limit state. Pier 4 presents values of safety indices less than one for both the scenarios analysed. On the contrary, piers 5 and 6 are characterized by safety indices values equal to 1 for the scenario 2 which represents a limit condition for safety checks while the results obtained for the scenario 3 show values less than one.

3.3 Evaluation of the seismic behaviour

To evaluate the seismic behaviour of the bridge multi-modal pushover analysis has been carried out following the approach described in previous Section 2 and considering scenarios 0 and 1 where the corrosion effects due to carbonation are applied on each pier of the bridge. According to as reported in Table 3, the maximum moment of the cross-section significantly decreases as a function of the corrosion level. Fig. 8 shows the trend of the moment-curvature diagram of the base gross-section of the pier 4 which clearly shows the correlation between the corrosion effects and the load-bearing capacity of the bridge. Furthermore, the corrosion process slightly influences the dynamic behaviour of the bridge. In fact, as a reduction of the pier's stiffness due to corrosion effects, the first natural periods are characterized by a slight increase. Table 7 shows the comparison of the fundamental vibration modes used for the execution of the multi-modal pushover analysis in terms of period and related participating mass.
Furthermore, no significant variations of the modal shapes occur considering the presence of corrosion effects (Fig. 9).

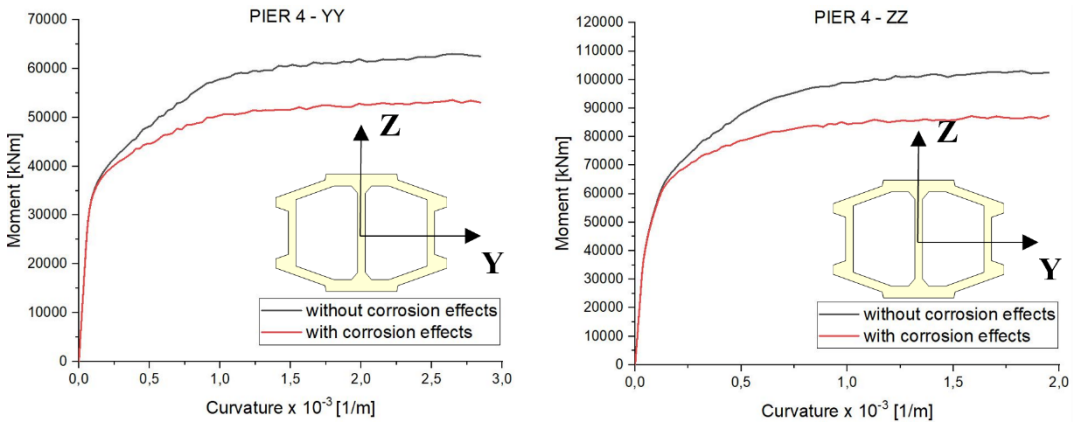

Figure 8. Pier 4 moment-curvature diagrams.

Table 7. Fundamental periods and related participating masses of the vibration modes used in the multi-modal pushover analysis.

scenario 0			
Mode [n°]	**Period [s]**	**Mass_TRAN_X [%]**	**Mass_TRAN_Y [%]**
1	3.37	0.17	17.38
2	3.22	22.87	0.97
4	2.31	2.38	4.13
6	2.02	0.36	1.79
7	1.91	1.17	2.73
8	1.64	5.10	1.42
10	1.42	11.06	0.37
12	1.23	0.55	7.21
13	1.21	1.19	0.83
14	1.19	0.55	3.57
16	1.06	8.40	2.17
18	1.05	0.07	1.53
19	1.02	6.02	0.05
20	1.01	2.36	2.24
23	0.97	1.47	5.18
26	0.93	0.32	9.93
35	0.88	0.03	1.23
38	0.86	2.25	2.17
42	0.86	1.32	1.39
43	0.86	1.19	0.04
49	0.85	1.06	1.15
scenario 1			
1	3.65	0.76	14.00
2	3.37	23.38	4.39
4	2.41	2.31	3.99
6	2.06	0.49	2.04
7	1.98	1.42	3.20
8	1.68	5.45	1.55
10	1.48	10.90	0.36
12	1.30	0.60	7.28
13	1.24	0.87	2.57
14	1.23	0.57	1.61
16	1.08	8.85	2.02
18	1.07	1.03	0.02
19	1.05	0.55	1.84
20	1.04	6.65	0.51
23	0.99	1.45	5.26
26	0.98	0.30	9.94
35	0.88	0.09	1.50
38	0.87	2.28	2.12
43	0.86	1.79	1.10
44	0.86	0.76	1.15
50	0.85	1.07	1.12

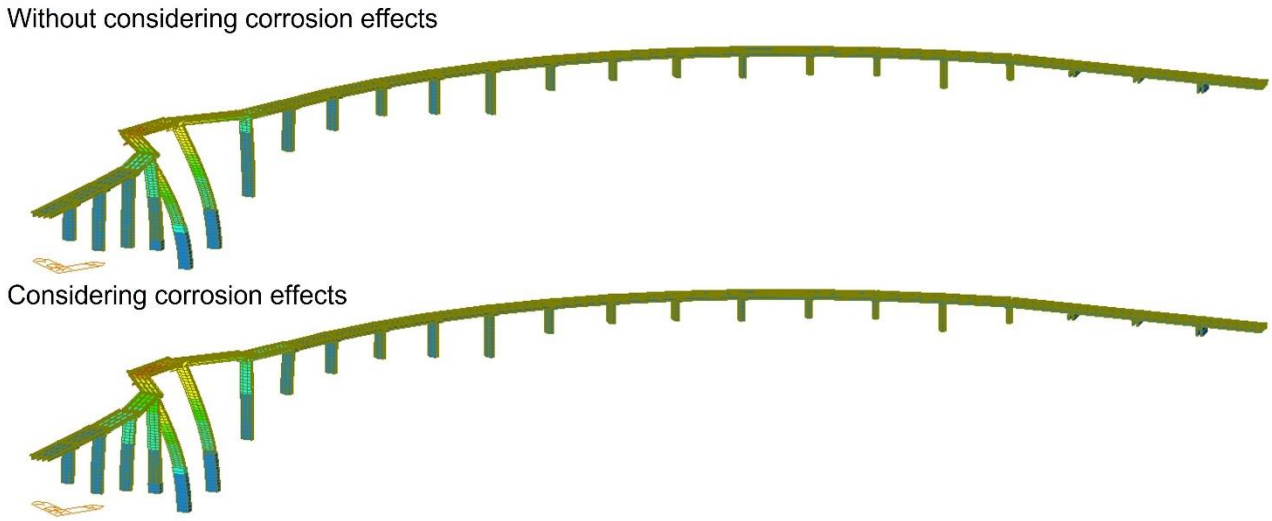

Figure 9. Comparison of the first vibration mode shape without considering and considering the presence of corrosion effects.

Several capacity curves have been obtained for the two scenarios analysed, each corresponding to a vibration mode shape characterized by participating mass equal or greater than 1% using a modal load profile. Capacity Spectrum Method (CSM) has been adopted for the evaluation of the performance point [52,53] which has been calculated taking into account the relevant seismic demand spectrum. As a consequence, for each considered vibration mode, it is possible to obtain the internal actions acting on the monitored structural elements in correspondence to the performance point. These internal actions have been combined using CQC (complete quadratic combination) rule for the safety structural checks. An iterative process has been carried out considering the increase of the demand spectrum up to the achievement of the required limit state. In this way, it is possible to evaluate the peak ground acceleration which lead to the collapse of the first monitored structural element (PGA_C) and the corresponding return period (RP_C) useful to obtain the following risk indices:

$$RI_{PGA} = \frac{PGA_C}{PGA_D} \tag{4}$$

$$RI_{RP} = \left(\frac{RP_C}{RP_D}\right)^{0.41} \tag{5}$$

where PGA_D is the design peak ground acceleration determined according to [35] and RP_D the related return period. Values close to one or larger than one characterizes cases where the risk level is acceptable. On the contrary, values close to zero characterizes high-risk cases.
Table 8 summarizes the results obtained for the ductile and brittle collapse mechanism, where X indicates the direction in correspondence to the longitudinal axis of the bridge and Y the correspondence transverse direction.
It is possible to notice that the value of ductile mechanism risk indices is the same for both the two directions due to the characteristics of the first vibration modes which involve a significant participating mass in X and Y direction.

Table 8. Risk indices.

	Ductile mechanism				Brittle mechanism			
	scenario 0		scenario 1		scenario 0		scenario 1	
	X	Y	X	Y	X	Y	X	Y
RI_{PGA}	3.17	3.17	2.72	2.72	2.02	1.84	1.58	1.43
RI_{RP}	5.01	5.01	4.05	4.05	2.68	2.35	1.89	1.65

The decrease of the value of the risk indices is evident if the corrosion effects are considered. Despite that values always greater than 1 have been obtained.
Starting from the value of risk indices reported in Table 8, it possible to determine the intervention time (IT) for the considered limit state (life-safety limit state in this work) using Eq. 4 [16]:

$$IT = 0.105 \cdot \frac{\min(RP)}{C_u} \tag{4}$$

where IT is the intervention time (in years), min(RP) is the minimum return which characterizes the obtained risk indices and C_u represents the use category coefficient considered equal to 2 [35]. In this case, the minimum value of risk index is obtained for the Y direction considering the brittle collapse mechanism, characterized by a return period equal to 3227 years which defines an intervention time equal to 169 years.

3.4 Retrofitting intervention

Considering the results obtained for the different scenarios described in previous Sections 3.1, 3.2 and 3.3, a retrofitting intervention involving the piers 4, 5 and 6 has been carried out in order to guarantee an adequate safety level of the bridge also in current configuration. In particular, piers cladding characterized by a thickness equal to 20 cm, have been realized having 92Ø16 longitudinal B450C steel rebars confined by Ø12/10 cm stirrups. The retrofitting intervention has been implemented in the FEM through the variation of the section properties of the beam elements representing the piers, according to as reported in Section 2 (Fig. 10). The construction phases of the proposed intervention have been illustrated in detail in Fig. 11.

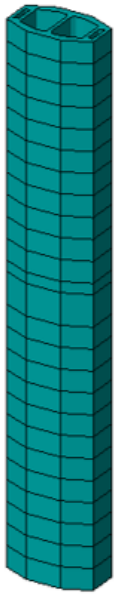

Figure 10. Retrofitting intervention of the pier 4: FEM implementation.

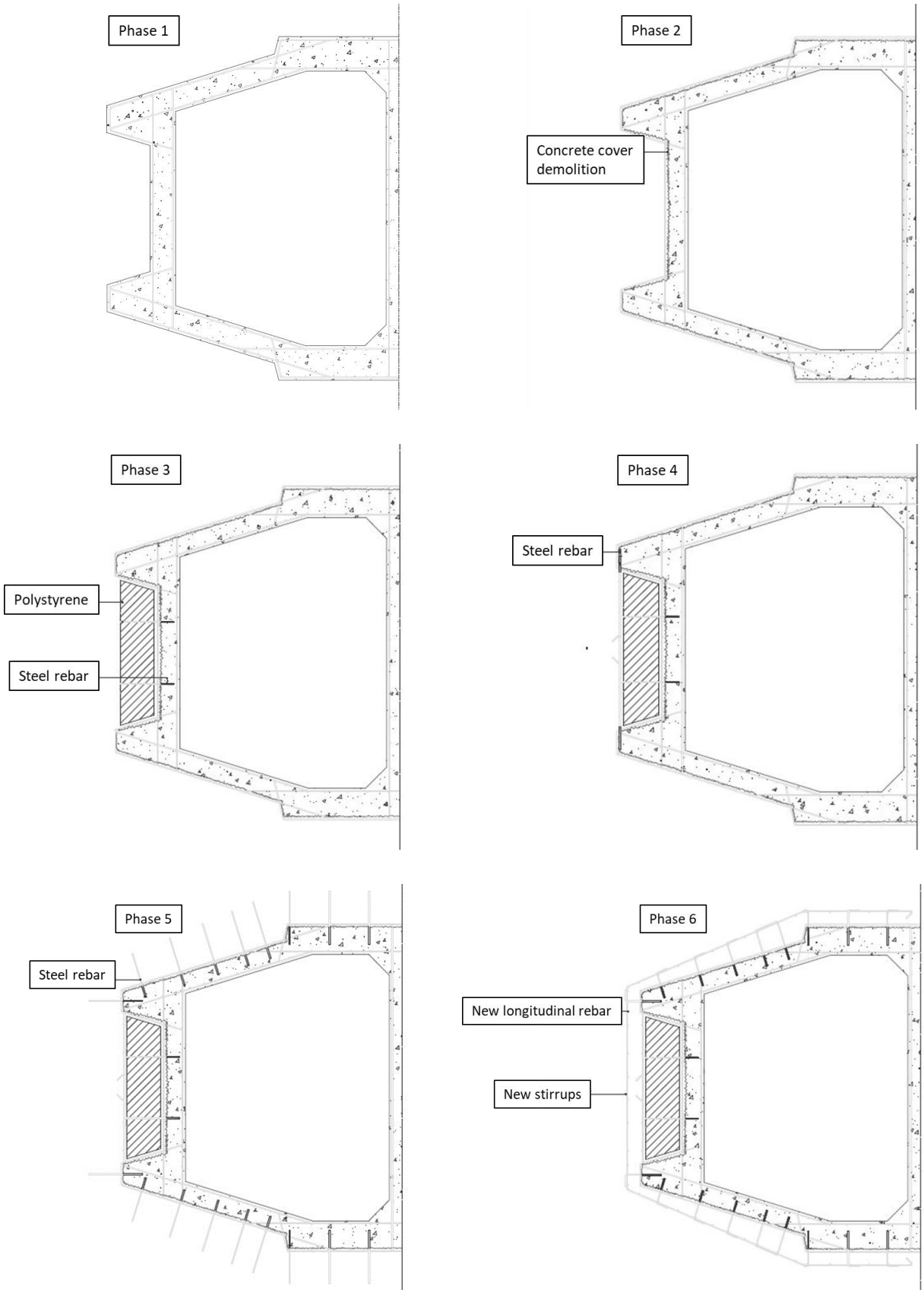

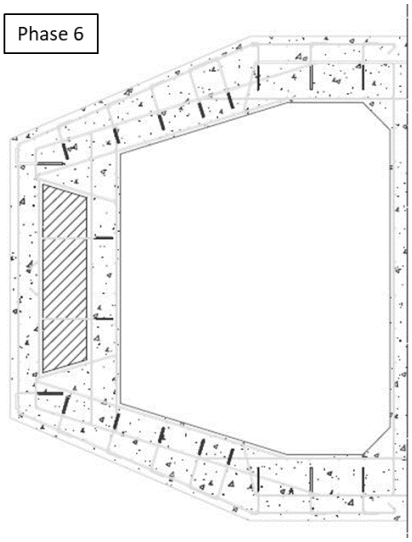

Figure 11. Construction phases of the retrofitting intervention.

Also in this case, the reduction of the gross-section bending stiffness of the piers due to concrete cracking has been taken into account, through the introduction of appropriate scale factor calculated as shown in Section 2. The load combinations considered for the analysis of the structural behaviour of the retrofitted configuration are the same described in Section 3.1, defined according to [35]. Table 9 summarizes the results, expressed in terms of safety indices, considering the scenario 2 (considered the worst-case scenario in terms of structural safety) with the execution of the retrofitting intervention.

Table 9. Range of the safety indices obtained for retrofitted configuration, considering the load combinations defined according to [35].

Pier 4	Pier 5	Pier 6
Sc2 (retrofitting intervention) [-] 0.12-0.59	Sc2 (retrofitting intervention) [-] 0.13-0.72	Sc2 (retrofitting intervention) [-] 0.12-0.64

The results show that the safety indices are characterized by values always lower than one, also considering the traffic loads acting on the three lanes.

4. Conclusions

In this paper, the structural behaviour of an existing RC bridge subjected to corrosion effects acting on some piers (in particular the piers 4, 5 and 6) is discussed. To evaluate the safety level of the bridge, four different scenarios have been analysed: (i) scenario 0, where the structural analyses has been carried out without taking into account the corrosion effects acting on the piers 4, 5 and 6, (ii) scenario 1, where the corrosion effects have been applied to all the steel reinforcements of the piers 4, 5 and 6, (iii) scenario 2, where the corrosion effects have been considered acting only in the steel reinforcements positioned in the inner perimeter of the hollow octagonal cross-section of the piers 4, 5 and 6 while the steel reinforcements of the outer perimeter are not considered in the structural checks and (iv) scenario 3, where the steel reinforcements of the inner perimeter of the hollow octagonal cross-section of the piers 4, 5 and 6 are not considered affected by corrosion effects and those of the outer perimeter are not considered in the structural checks. The structural analyses have been carried out taking into account an efficient approach where the main structural elements of the

bridge (piers, pier caps and deck) have been introduced in the FEM using only Timoshenko beam elements while the corrosion effects due to carbonation has been taken into account as reduction of steel reinforcements diameters. The results have shown an inadequate safety level of the structure especially in the presence of traffic loads. For this reason, a transient configuration has been analysed considering a reduction of the traffic loads acting on the existing RC bridge, to evaluate the possibility of maintaining the operativity of the structure.
In addition, the seismic performance of the bridge has been studied in detail using multi-modal pushover approach and considering scenarios 0 and 1 where the corrosion effects are considered acting on all the piers of the bridge at the same time. The results obtained have been summarizes with appropriate risk indices expressed in terms of peak ground acceleration and related return period and have shown that, de-spite the reduction of these indices as a function of corrosion effects, the analysed bridge is not characterized by a significant vulnerability under seismic action.
Finally, a retrofitting intervention on piers 4, 5 and 6, which consists in the realization of piers cladding characterized by a thickness equal to 20 cm and having 92Ø16 longitudinal B450C steel rebars confined by Ø12/10 cm stirrups, has been proposed to guarantee an adequate safety level of the bridge under all the load combinations defined by [35].

References

[1] Tan, J.S.; Elbaz, K.; Wang, Z.H.; Shen, J.S.; Chen, J. Lessons learnt from bridge collapse: a view of sustainable management. Sustainability 2020, 12(3), 1205.

[2] Domaneschi, M.; Pellecchia, C.; De Iuliis, E.; Cimellaro, G.P.; Morgese, M.; Khalil, A.A.; Ansari, F. Collapse analysis of the Polcevera viaduct by the applied element method. Engineering Structures 2020, 214, 110659.

[3] Bazzucchi, F.; Restuccia, L.; Ferro, G.A. Considerations over the Italian road bridge infrastructure safety after the Polcevera viaduct collapse: past errors and future perspectives. Frattura ed Integrità Strutturale 2018, 46, 400-421.

[4] Fan, Y.; Zhu, J.; Pei, J.; Li, Z.; Wu, Y. Analysis for Yangmingtan Bridge collapse. Engineering Failure Analysis 2015, 56, 20-27.

[5] Crespi, P.; Zucca, M.; Valente, M.; Longarini, N. Influence of corrosion effects on the seismic capacity of existing RC bridges. Engineering Failure Analysis 2022, 140, 106546.

[6] Miluccio, G.; Losanno, D.; Parisi, F.; Cosenza, E. Traffic-load fragility models for prestressed concrete girder decks of existing Italian highway bridges. Engineering Structures 2021, 249, 113367.

[7] Nuti, C.; Briseghella, B.; Chen, A.; Lavorato, D.; Iori, T.; Vanzi, I. Relevant outcomes from the history of Polcevera Viaduct in Genova, from design to nowadays failure. Journal of Civil Structural Health Monitoring 2020, 10(1), 87-107.

[8] Deng, L.; Wei, W.; Yu, Y. State-of-The-Art review on the causes and mechanisms of bridge collapse. Journal of Performance of Constructed Facilities 2016, 30(2), 04015005.

[9] De Domenico, D.; Messina, D.; Recupero, A. Seismic vulnerability assessment of reinforced concrete bridge piers with corroded bars. Structural Concrete 2023, 24(1), 56-83.

[10] Zanini, M.A.; Pellegrino, C.; Morbin, R.; Modena, C. Seismic vulnerability of bridges in transport networks subjected to environmental deterioration. Bulletin of Earthquake Engineering 2013, 11(1), 561-579.

[11] Do-Eun, C.; Gardoni, P.; Rosowsky, D.; Haukaas, T. Seismic fragility estimates for reinforced concrete bridges subject to corrosion. Structural Safety 2009, 31(4), 275-283.

[12] Mahboubi, S.; Kioumarsi, M. Damage assessment of RC bridges considering joint impact of corrosion and seismic loads: A systematic literature review. Construction and Building Materials 2021, 295, 123662.

[13] Zhao, J.; Lin, Y.; Li, X.; Meng, Q. Experimental study on the cyclic behavior of reinforced concrete bridge piers with non-uniform corrosion. Structures 2021, 33, 999-1006.

[14] Crespi, P.; Zucca, M.; Valente, M. On the collapse evaluation of existing RC bridges exposed to corrosion under horizontal loads. Engineering Failure Analysis 2020, 116, 104727.

[15] Gardoni, P.; Mosalam, K.; Der Kiureghian, A. Probabilistic seismic demand models and Fragility estimates for RC bridges. Journal of Earthquake Engineering 2003, 7, 79-106.

[16] Zucca, M.; Crespi, P.; Stochino, F.; Puppio, M.L.; Coni, M. Maintenance interventions period of existing RC motorway viaducts located in moderate/high seismicity zones. Structures 2023, 47, 976-990.

[17] Pelle, A.; Briseghella, B.; Bergami, A.V.; Fiorentino, G.; Giaccu, G.F.; Lavorato, D.; Quaranta, G.; Rasulo, A.; Nuti, C. Time-dependent cyclic behavior of reinforced concrete bridge columns under chlorides-induced corrosion and rebars buckling. Structural Concrete 2022, 23, 81-103.

[18] Kumar, R.; Gardoni, P.; Sanchez-Silva, M. Effect of cumulative seismic damage and corrosion on the life-cycle cost of reinforced concrete bridges. Journal of Earthquake Engineering 2009, 38, 887-905.

[19] Ou, Y.C.; Fan, H.D.; Nguyen, N.D. Long-term seismic performance of reinforced concrete bridges under steel reinforcement corrosion due to chloride attack. Journal of Earthquake Engineering 2013, 42, 2113-2127.

[20] Fan, W.; Sun, Y.; Yang, C.; Sun, W.; He, Y. Assessing the response and fragility of concrete bridges under multi-hazard effect of vessel impact and corrosion. Engineering Structures 2020, 225, 111279.

[21] Yuan, W.; Guo, A.; Li, H. Seismic failure mode of coastal bridge piers considering the effects of corrosion-induced damage. Soil Dynamics and Earthquake Engineering 2017, 93, 135-146.

[22] Yuan, W.; Guo, A.; Yuan, W.; Li, H. Shaking table tests of coastal bridge piers with different levels of corrosion damage caused by chloride penetration. Construction and Building Materials 2018, 173, 160-171.

[23] Ma, Y.; Che, Y.; Gong, J. Behavior of corrosion damaged circular reinforced concrete columns under cyclic loading. Construction and Building Materials 2012, 29, 548-556.

[24] Zhou, H.; Chen, S.; Du, Y.; Lin, Z.; Liang, X.; Liu, J.; Xing, F. Field test of a reinforced concrete bridge under marine environmental corrosion. Engineering Failure Analysis 2020, 115, 104669.

[25] Biondini, F.; Camnasio, E.; Palermo, A. Lifetime seismic performance of concrete bridges exposed to corrosion. Structure and Infrastructure Engineering 2014, 10, 880-900.

[26] Papé, T.M.; Melchers, R.E. The effects of corrosion on 45-year-old pre-stressed concrete bridge beams. Structure and Infrastructure Engineering 2011, 7, 101-108.

[27] Akiyama, M.; Frangopol, D.M.; Ishibashi, H. Toward life-cycle reliability-, risk- and resilience-based design and assessment of bridges and bridge networks under independent and interacting hazards: emphasis on earthquake, tsunami and corrosion. . Structure and Infrastructure Engineering 2020, 16, 26-50.

[28] Bossio, A.; Fabbrocino, F.; Monetta, T.; Lignola, G.P.; Prota, A.; Manfredi, G.; Bellucci. F. Corrosion effects on seismic capacity of reinforced concrete structures. Corrosion Reviews 2018, 37, 45-46.

[29] Stefanoni, M.; Angst, U.; Elsener, B. Corrosion rate of carbon steel in carbonated concrete – A critical review. Cement and Concrete Research 2018, 103, 35-48.

[30] Almusallam, A.A. Effect of degree of corrosion on the properties of reinforcing steel bars. Construction and Building Materials 2001, 15, 361-368.

[31] Lin, W.T.; Wu, Y.C.; Cheng, A.; Lee T.Y. Seismic response for a reinforce concrete specimen considering corrosive hazards. Applied Mechanics and Materials 2015, 764-765, 1124-1128.

[32] Cui, F.; Zhang, H.; Ghosn, M.; Xu, Y. Seismic fragility analysis of deteriorating RC bridge substructures subject to marine chloride-induced corrosion. Engineering Structures 2018, 155, 61-72.

[33] De Domenico, D.; Messina, D.; Recupero, A. Quality control and safety assessment of prestressed concrete bridge decks through combined field tests and numerical simulation. Structures 2022, 39, 1135-1157.

[34] Li, H.; Li, L.; Zhou, G.; Xu, L. Time-dependent seismic fragility assessment for aging highway bridges subject to non-uniform chloride-induced corrosion. Journal of Earthquake Engineering 2022, 26(7), 3523-3553.

[35] Decreto Ministeriale 17/01/2018, Ministero delle Infrastrutture e dei Trasporti, G.U. Serie Generale n.42 del 20/02/2018 – S.O.8.

[36] MIDAS Civil, Analysis Reference, 2022.

[37] EN 1337-3:2005. Structural bearings – Part 3: Elastomeric bearings. CEN (European Committee for Standardization), Management Centre. Brussels.

[38] EN 1998-3:2005. Eurocode 8: Design of structures for earthquake resistance – Part 3: Assessment and retrofitting of buildings. CEN (European Committee for Standardization), Management Centre. Brussels.

[39] Chen, W.F.; Duan, L. Bridge Engineering – Seismic Design, CRC Press, Boca Raton, FL, 2000.

[40] EN 1998-2:2005. Eurocode 8: Design of structures for earthquake resistance – Part 2: Bridges. CEN (European Committee for Standardization), Management Centre. Brussels.

[41] Kent, D.C.; Park, R. Flexural members with confined concrete. Journal of the Structural Division 1971, 97, 1969-1990.

[42] Park, R.; Paulay, T. Reinforced Concrete Structures, John Wiley and Sons, New York, 1975.

[43] FEMA 356. Prestandard and commentary for the seismic rehabilitation of buildings. Federal Emergency Management Agency: Washington, DC.

[44] FEMA 440. Improvement of nonlinear static seismic analysis procedure. Applied Technology (ATC-55 Project) Department of Homeland Security, Federal Emergency Management Agency: Washington, DC.

[45] Roy, S.K.; Poh, K.B; Northwood, D. Durability of concrete—accelerated carbonation and weathering studies. Building and Environment 1999, 34, 597-606.

[46] Saetta, A.; Vitaliani, R. Experimental investigation and numerical modeling of carbonation process in reinforced concrete structures: Part I: Theoretical formulation. Cement and Concrete Research 2004, 34, 571-579.

[47] Bertolini, L.; Elsner, B.; Pedeferri, B.; Polder, R. Corrosion of steel in concrete, prevention, diagnosis and repair. Wiley-VCH, Weinheim, 2004.

[48] BRITE EURAM PROJECT BE 95-1347. Duracrete – probabilistic performance-based durability design of concrete structures.

[49] Berto, L.; Vitaliani, R.; Saetta, A.; Simioni, P. Seismic assessment of existing RC structures affected by degradation phenomena. Structural Safety 2009, 31, 284-297.

[50] Melchers, R.E. Modelling durability of reinforced concrete structures. Corrosion Engineering. Science and Technology 2020, 55, 171-181.

[51] Wan, X.; Wittmann F.H.; Zhao, T. Influence of mechanical load on service life of reinforced concrete structures under dominant influence of carbonation. Restoration of Buildings and Monuments 2011, 17, 103-110.

[52] ATC-40:1996. Seismic Evaluation and Retrofitting of Concrete Buildings. Applied technology council, 8.1-8.66, Redwood City, CA, 1996.

[53] Causevic, M.; Mitrovic, S. Comparison between non-linear dynamic and static seismic analysis of structures according to European and US provisions. Bulletin of Earthquake Engineering 2011, 9(2), 467-489.